Chemical Engineering Journal 117 (2006) 117–122

Chemical Engineering Journal

www.elsevier.com/locate/cej

Comparison of mean drop sizes and drop size distributions in agitated liquid–liquid dispersions produced by disk and open type impellers

D. Sechremeli, A. Stampouli, M. Stamatoudis *

Department of Chemical Engineering, Aristotle University of Thessaloniki, Greece

Received 5 July 2005; received in revised form 15 October 2005; accepted 19 December 2005

Abstract

A comparison is made of drop diameters produced by a disk and an open type six-blade impeller having the same impeller diameter and width and rotated at the same speed. Drop size measurements in situ at 200, 250, 300, 350, 400 and 450 rpm and at hold-up fractions 0.01, 0.025, 0.05 and 0.10 showed that always the Sauter mean drop diameters produced by the open style impeller were 6–82% larger than the ones produced by the disk impeller. Plots of $\ln d_{32}$ versus $\ln N$ and $\ln d_{\max}$ versus $\ln N$ gave straight lines. Plots of d_{32} versus $d_{\max}$ gave relationships not quite linear.

Keywords: Agitated dispersion; Drop size distribution; Liquid–liquid dispersion; Disk type impeller; Open type impeller

1. Introduction

An important factor determining the interphase reaction rate and the mass transfer rate between two immiscible liquid phases is the interfacial area. Many operations in chemical engineering require the contact of two liquid phases between which mass and heat transfer with reaction occurs. Thus, it is very important for designing various operations including the design of two-phase rectors to be able to describe correctly agitated dispersions. One industrially important method of obtaining large interfacial areas is agitation. Agitating two immiscible liquids results into the production of a dispersion of one phase into the other in the form of small droplets. A review of this important area is given by Tavlarides and Stamatoudis [1].

It is well known that the drop size distribution in an agitated dispersion is a result of the dynamic equilibrium that exists between the breaking and coalescing drops. Decreasing the drop breakage rate or increasing the drop coalescence rate results in greater drops. Conversely, increasing the drop breakage rate or decreasing the drop coalescence rate results in smaller drop sizes. This dynamic state can be described by a mathematical model using population balances equations.

In a dynamic flow field the maximum size of a drop is determined by the external deforming forces and the restoration forces [2]. The external deforming forces are the result of turbulent fluctuations and the viscous stress due to the velocity gradients in the surrounding field. The restoring forces are the result of the interfacial tension and/or the internal viscous stress. The maximum stable drop in a turbulent field depends on the turbulent field itself and on the force that holds the drops together. Kolmogoroff [3] and Hinze [4] assumed that in order for a drop to become unstable and break, the kinetic energy of the drop oscillations must be sufficient to overcome the surface force holding the drop together. Thus, the Weber number, N_{We}, which is defined as the ratio of the kinetic energy to the surface energy, has a critical value above which the drop becomes unstable. In locally isotropic turbulent flows

$$(N_{We})_{\text{crit}} = \frac{c\rho_c \varepsilon^{2/3} d_{\max}^{5/3}}{\sigma} = \text{constant} \tag{1}$$

where c is a constant, ρ_c the continuous phase density, ε the rate of energy dissipating per unit mass of the liquid, $d_{\max}$ the maximum stable drop in the dispersion and σ is the interfacial tension. Eq. (1) holds for low dispersed phase viscosity, drops larger than Kolmogorov microscale, and when coalescence is negligible.

The maximum stable drop that can exist is obtained from Eq. (1) and for a given system is

$$d_{\max} \propto \varepsilon^{-2/5} \tag{2}$$

* Corresponding author.
E-mail address: stamatou@auth.gr (M. Stamatoudis).

1385-8947/$ – see front matter
doi:10.1016/j.cej.2005.12.015

Nomenclature

A_{max}	a constant of Eq. (6) (μm)
c	a constant of Eq. (1)
C_1	a constant of Eq. (6)
d	drop diameter (μm)
d_i	drop diameter in the interval i (μm)
d_{max}	the experimental maximum drop diameter of the sample (μm)
d_{min}	the droplet diameter above which prevention of coalescence becomes effective (μm)
d_{32}	Sauter mean diameter $(\sum n_i d_i^3)/(\sum n_i d_i^2)$ (μm)
D	impeller diameter (cm)
D_d	disk diameter (cm)
D_L	length of impeller blade (cm)
D_W	width of impeller blade (cm)
$f(d)\,dd$	number fraction of drops of diameter between d and $d + dd$
$G(d)$	cumulative drop number or volume distribution function (defined in Eq. (6))
n_i	number of drops of diameter d_i
N	impeller rotational speed (min^{-1})
N_{Po}	impeller power number ($P/\rho N^3 D^5$)
N_{Re}	impeller Reynolds number ($\rho N D^2/\mu$)
P	impeller power (W)
T	tank diameter (cm)
x_b	blade thickness (cm)
x_d	disk thickness (cm)

Greek letters

ε	turbulent energy dissipation per unit mass (m^2/s^3)
ε_{aver}	average turbulent energy dissipation per unit mass (m^2/s^3)
ε_{max}	maximum turbulent energy dissipation per unit mass (m^2/s^3)
ϕ	hold-up fraction (m^3 of dispersed phase/m^3 of dispersion)
μ_d	dispersed phase viscosity (Pa s)
ρ_c	continuous phase density (g/cm^3)
ρ_d	dispersed phase density (g/cm^3)
σ	interfacial tension (N/m)
σ_{st}	standard deviation

Sprow [5] showed that

$$d_{32} \propto d_{max} \tag{3}$$

In an agitated vessel the average energy dissipation, ε_{aver} (=$P/\rho V_T$), is usually used. Here P is the power transferred to the fluid in the vessel by the impeller, ρ the density of the fluid and V_T is the volume of the fluid in the vessel. Since at $N_{Re} > 10{,}000$, $P \propto N^3 D^5$ [6,7].

$$\varepsilon_{aver} \propto N^3 D^2 \tag{4}$$

Thus,

$$d_{32} \propto N^{-6/5} \tag{5}$$

Zhou and Kresta [8] found that the assumption that d_{32} is directly proportional to d_{max} is not always valid. In addition, they found that a better correlation for d_{32} is obtained by using both the maximum turbulence energy dissipation rate per unit mass, ε_{max}, instead of average energy dissipation, ε_{aver}, and the effect of mean flow (circulation time). In the past, most of the work has been focused on studying the drops formed by a flat vertical six-blade disk style (turbine type) impeller. Daglas and Stamatoudis [9] found that besides geometry of the impeller, its vertical position also plays a role in determining the drop size distribution. Fernandes and Sharma [10] conducted experiments comparing the interfacial area produced by various types impellers. Their results showed that the greater area was produced by the flat vertical six-blade disk style impeller followed by the flat vertical six-blade open style one. Brown and Pitt [11] found that the impeller geometry (different proportions D_W/D) does not influence mean drop sizes when the impeller diameter and the rotational speed are the same. Zhou and Kresta [2] investigated the drop size distribution for very dilute ($\phi = 0.0003$) liquid–liquid dispersions for Rushton type turbine and for three axial flow impellers. No comparison between them is shown. Pacek et al. [12] studied the mean drop sizes and drop size distributions produced by two disk type impellers and by four low power number impellers. They found that the last impellers gave similar sized drops, which were much smaller than those found by the two disk type impellers. No work has been done in the literature systematically comparing the mean drop sizes and the drop size distributions produced by the flat vertical six-blade disk style impeller and the flat vertical six-blade open style one.

The purpose of this work is to compare systematically the droplet dispersion ability of the flat vertical six-blade disk style impeller and the flat vertical six-blade open style one when both have the same impeller diameter and width and are rotated at the same rotational speed.

2. Experimental

The main experimental apparatus consisted of a vessel, the impellers and the agitator. Fig. 1 shows a schematic drawing of this experimental apparatus. The cylindrical glass vessel had a $T = 30$ cm inside diameter (with a very slight flair at the two ends) and a height of 30.5 cm. Four vertical baffles (width = $T/10$) were equally spaced around the periphery of the vessel. The top and the bottom plates were made of aluminum. The impeller shaft was inserted through a 3.9 cm inside diameter cylinder fitted on the top plate. The liquid level in this cylinder was 2–3 cm above the liquid level inside the vessel in order to prevent air entrainment. The 2.5 cm diameter impeller shaft was moved by a 0.37 kW agitator (type Rd 10.12 V, FLUID, Germany). This agitator had a variable speed drive. The two impellers used were positioned in the center of the vessel. The two impellers (shown in Fig. 2) had the same diameter but different geometry. They

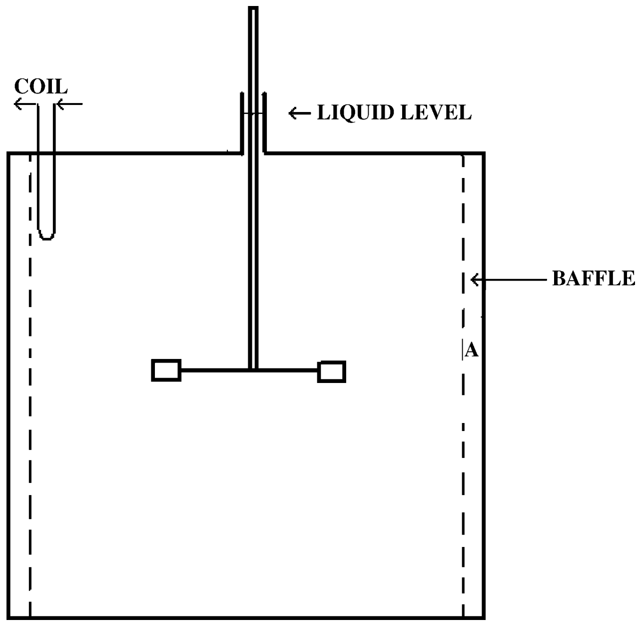

Fig. 1. Schematic diagram of the stirred vessel.

had the following characteristics: (a) flat vertical six-blade disk style ($D = 10$ cm, $D_W = D/5$, $D_L = D/4$, $D_d = 2/3D$, $x_d = 0.15$ cm, $x_b = 0.12$ cm); (b) flat vertical six-blade open style ($D = 10$ cm, $D_W = D/5$). The vessel liquids were maintained at $25 \pm 0.1\,^{\circ}$C by regulating the temperature of the water passing through a coil. A Julabo PC circulator achieved the regulation of the water temperature.

The dispersion had distilled water as the continuous phase and kerosene as the dispersed phase. The dispersed phase had a viscosity $\mu_d = 0.00093$ Pa s and a density of $\rho_d = 0.794$ g/cm^3). The interfacial tension was $\sigma = 0.0387$ N/m. The viscosity was measured by Cannon-Fenske viscometers and the interfacial tension by a Du Nouy type tensiometer. Experiments were conducted at hold-up fractions $\phi = 0.01$, 0.025, 0.05 and 0.1. The impeller speeds studied were 200, 250, 300, 350, 400 and 450 rpm (with the impeller Reynolds number, N_{Re}, ranging from 39,000 to 87,000). The impeller rotational speed was measured by a 725 DIGI-BETA stroboscope (Mayer and Wonisch, Germany). The lower rotational speed limit was set as to have enough agitation to result in the dispersion of all the organic phase into the water phase.

Drop size distributions were measured in situ using photomicrography. Photographs were taken at a position A, located 0.5 cm behind the glass wall and 4 cm above the center of the vessel. Even though the drop size distribution depends on the position of measurement [9], this position was chosen in order to obtain pictures even at the high hold-up fraction of $\phi = 0.1$. No data were taken far away from the impeller. For good light illumination purposes, a 2 cm × 4 cm mirror was attached on a baffle 1 cm behind the glass wall at the position of photographing. The presence of mirrors was necessary in order to photograph dense dispersions. The light flashes were directed towards the mirror and then were reflected back and into a stereoscope. The drops were viewed through a Sz-Tr Olympus Zoom Stereo Microscope and photographs were taken by a camera attached to it. The camera shutter was kept opened and the electronic flash unit (the previously described stroboscope) was triggered at prescribed times. Enough photographs were taken so as to make samples of at least 500 drops. The slides were projected on a screen and the drop sizes were measured with known magnification. The magnification ratio was found by photographing a wire of known diameter. It was estimated that the maximum experimental error in drop diameter measurement was around 5%. This was estimated from the uncertainty in measuring the drop on the screen by a ruler. The maximum drop diameter found in each sample, d_{max}, was also determined.

It was observed that the drop size distribution in the dispersion continues to undergo changes even after a long stirring time. A time of 90 min was found to be sufficient for obtaining equilibrium state (unchanging d_{32}) at all experimental conditions.

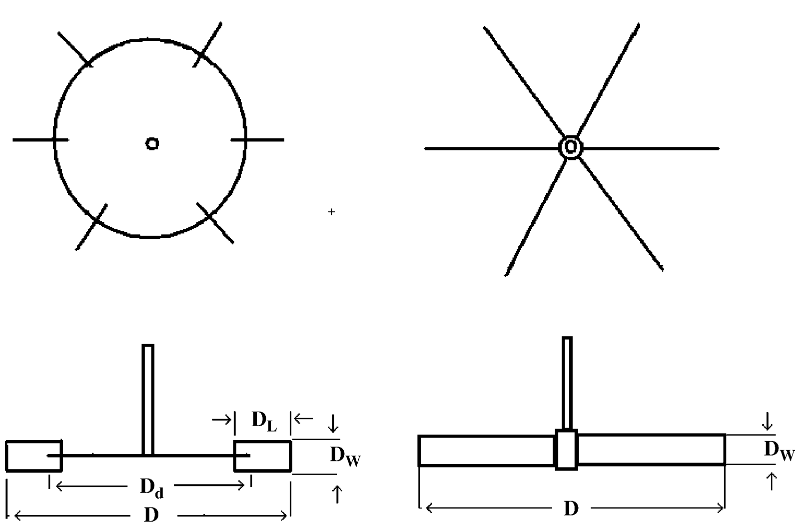

Fig. 2. Schematic diagram of (A) disk type impeller and (B) open type impeller.

Table 1
Sauter mean and maximum drop diameters (μm) for various rotational speeds and hold-up fractions

rpm	Disk style		Open style	
	α_{32}	α_{max}	α_{32}	α_{max}
$\phi = 0.01$				
200	136	350	238	429
250	127	320	202	378
300	107	298	179	312
350	99	286	170	295
400	89	274	150	288
450	86	242	137	268
$\phi = 0.025$				
200	290	525		
250	250	458		
300	221	422	402	649
350	195	332	339	559
400	165	298	291	492
450	150	258	266	465
$\phi = 0.05$				
250	378	571		
300	289	493	427	748
350	280	441	386	651
400	253	417	358	585
450	235	397	309	521
$\phi = 0.10$				
250	468	715		
300	401	695	439	846
350	348	558	391	749
400	309	515	356	656
450	296	469	314	559

3. Results and discussion

Many experiments were conducted. Table 1 shows the experimental results for the Sauter mean drop diameter, d_{32}, and the maximum drop diameter, d_{max}, for both impellers at various impeller speeds and hold-up fractions.

It is observed that drops produced by the open style impeller are between 6 and 82% larger than the ones produced by the disk one at the same hold-up fraction and rotational speed. This is expected because the impeller Reynolds number of this work (N_{Re} = 39,000–87,000) corresponds to a power number $N_{Po} = 5$ for the disk style impeller and to $N_{Po} = 4$ for the open style one [7]. The greater power number (greater average energy dissipation) for the disk impeller results into greater maximum turbulence energy dissipation rate per unit mass, ε_{max} [8], and thus greater drop breakage rates and/or smaller coalescence rates. The difference in the drop sizes produced by the two impellers diminishes at higher hold-up fraction. This again is a result of greater coalescence rates as the hold-up fraction increases. Thus, greater rotational speeds are necessary for the open style impeller in comparison with the disk type one to achieve the same drop sizes. The differences of the drop sizes produced by the two impellers is better seen from the drop size distributions measured at various hold-up fractions and rotational speeds. Fig. 3 compares the drop size distributions produced by the two impellers for $\phi = 0.025$ and $N = 300$ rpm. Similarly Fig. 4 compares the drop size distributions produced by the two impellers for $\phi = 0.10$ and $N = 400$ rpm. In this figure there is a tendency to form bimodal distribution for both impellers. This is expected due to higher dispersed phase hold-up fraction (resulting into greater coalescence rates). In addition, the greater coalescence rates at higher hold-up fractions results into the drop size distribution curves of Fig. 4 being closer than the ones of Fig. 3. The drop size distributions shown in these graphs and the ones for other hold-up fractions and rotational speeds (not shown here) clearly indicate different drop size distributions for the two impellers at the same hold-up fraction and rotational speed. It is observed that the drop size distribution produced by the disk type impeller is always taller and to the left of the distribution produced by the open style one. In other words, for the same hold-up fraction, impeller diameter and width and rotational speed, the drops produced by the disk type impeller were smaller and more uniform than the ones produced by the open style one. This greater dispersion ability of disk type impeller in agitated dispersions was also observed by Fernandes and Sharma [10]. They noticed that the disk type impeller produces greater interfacial area than

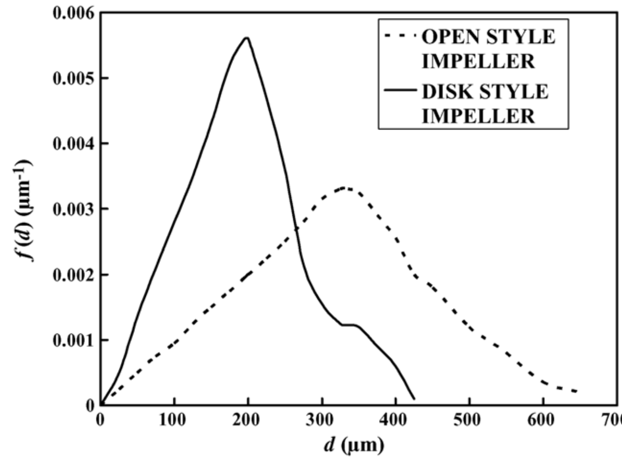

Fig. 3. Drop size distributions produced by a disk and an open type impeller for $\phi = 0.025$ and $N = 300$ rpm.

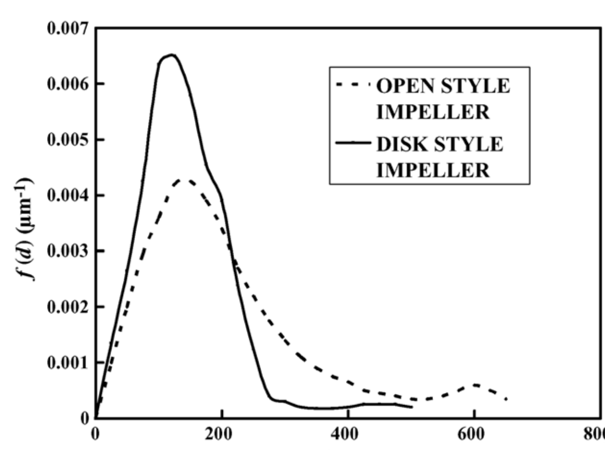

Fig. 4. Drop size distributions produced by a disk and an open type impeller for $\phi = 0.10$ and $N = 400$ rpm.

the open type one. The results of this work are contrary to the ones of Brown and Pitt [11] who found that the impeller geometry (different proportions D_W/D) does not influence mean drop sizes when the impeller diameter and the rotational speed are the same.

The experimental drop size distribution was fitted with several standard size distributions of the literature [13]. Following the best distribution was selected as the one that gave the most accurate mean. This was achieved by minimizing the variance of the mean size [13]. The relatively best distributions fitting the experimental distributions of this work were found to be the upper limit volume distribution and the normal number distribution. The cumulative drop volume distribution [13] is given by

$$G(d) = \frac{1}{\sigma_{st}\sqrt{2\pi}} \int_{-\infty}^{\ln d} \times \exp\left(-\frac{[\ln\{C_1 d\} - (A_{max} - d)]^2}{2\sigma_{st}^2}\right) d(\ln d) \qquad (6)$$

where σ is the standard deviation, A_{max} the upper limit for d (in this work taken as 1.2 times d_{max}, the largest measured diameter of the sample) and C_1 is a constant.

Figs. 5–8 show plots of $\ln d_{32}$ versus $\ln N$ and of $\ln d_{max}$ versus $\ln N$ (with their respective slopes) for both impellers at $\phi = 0.01$, 0.025, 0.05 and 0.10, respectively. From these figures good linear correlations ($R^2 = 0.93$–1.00) are observed for both impellers. The line of $\ln d_{32}$ versus $\ln N$ for all experiments conducted gave slopes ranging from −0.61 to −0.82 for the disk type impeller and from −0.66 to −1.03 for the open one. Also, the line $\ln d_{max}$ versus $\ln N$ gave slopes ranging from −0.41 to −0.89 for the disk type impeller and from −0.58 to −1.01 for the open one. The slopes for $\phi = 0.01$ are lower than those of other hold-up fraction. No other trend in the slopes is observed. Shinnar [14] derived that in the impeller region, where the breakage phenomena predominates, the line $\ln d_{max}$ versus $\ln N$ has a slope of −1.2 for drops larger than Kolmogorov microscale and −1.5 for drops smaller than Kolmogorov microscale. In the region away from the impeller where coalescence phenomena predominate the slope of $\ln d_{min}$ versus $\ln N$ should be −0.75. Apparently in this work the slopes obtained are a result of data taken away from the impeller region where the breakage rate is controlling and in the region where both coalescence and breakage play a significant role in determining the drop size distribution.

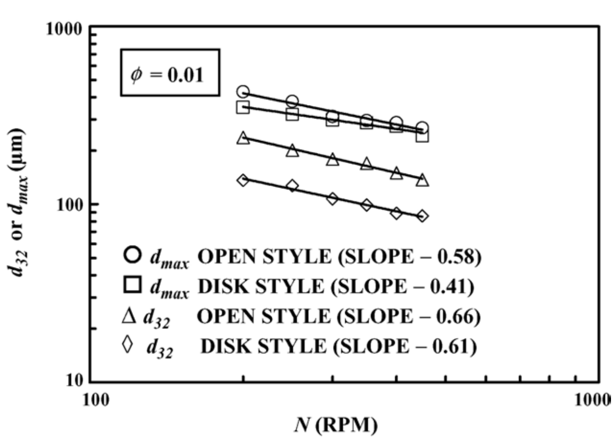

Fig. 5. Plots of $\ln d_{32}$ vs. $\ln N$ and of $\ln d_{max}$ vs. $\ln N$ for disk and open type impellers at $\phi = 0.01$.

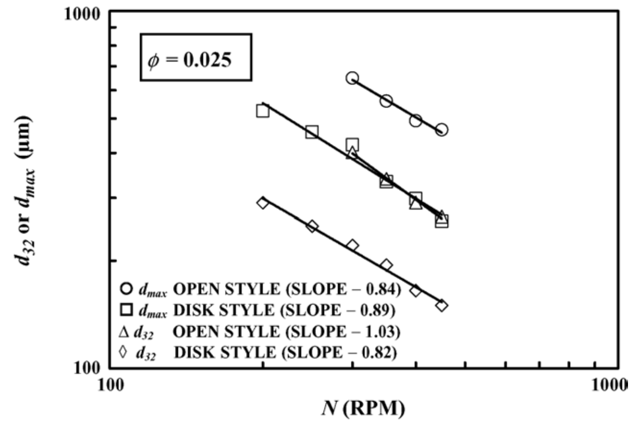

Fig. 6. Plots of $\ln d_{32}$ vs. $\ln N$ and of $\ln d_{max}$ vs. $\ln N$ for disk and open type impellers at $\phi = 0.025$.

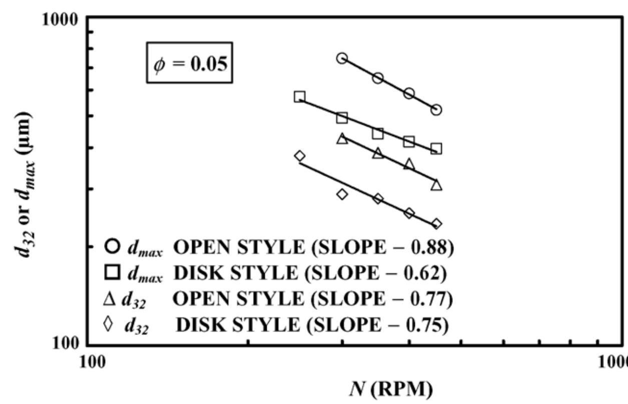

Fig. 7. Plots of $\ln d_{32}$ vs. $\ln N$ and of $\ln d_{max}$ vs. $\ln N$ for disk and open type impellers at $\phi = 0.05$.

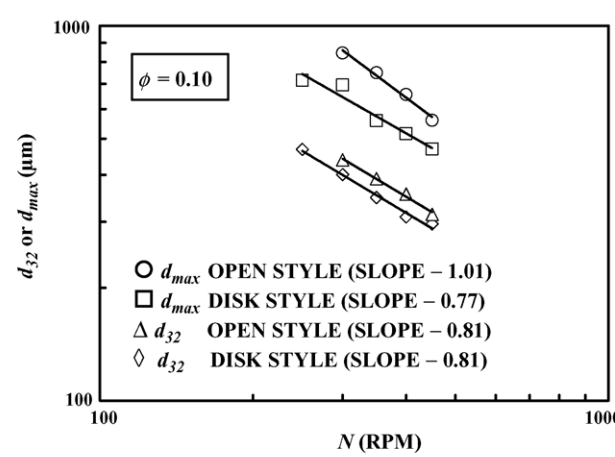

Fig. 8. Plots of $\ln d_{32}$ vs. $\ln N$ and of $\ln d_{max}$ vs. $\ln N$ for disk and open type impellers at $\phi = 0.10$.

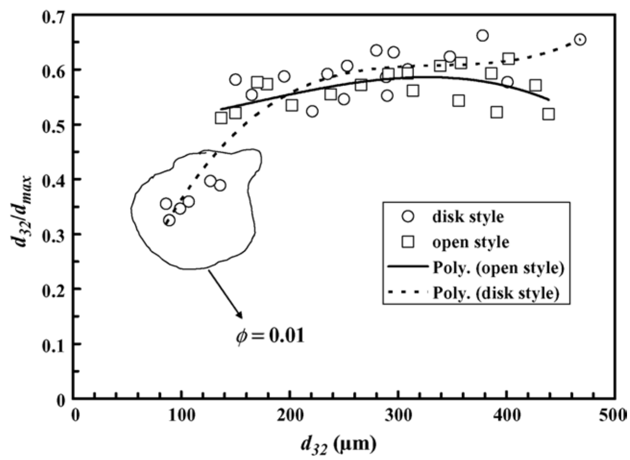

Fig. 9. Plots of d_{32}/d_{max} vs. d_{32} for the disk and open style impellers for all hold-up fractions and impeller speeds studied.

Fig. 9 shows the plots of d_{32}/d_{max} versus d_{32} for the disk and open style impellers for all hold-up fractions and impeller speeds studied in this work. As it is seen, the d_{32}/d_{max} ratio, with the exception of that corresponding to the disk impeller and $\phi = 0.01$, it ranges between 0.51 and 0.66. On the other hand, the d_{32}/d_{max} ratio for the disk impeller and $\phi = 0.01$ ranges between 0.32 and 0.40. All points are scattered. This is expected because the d_{max} is impossible to be measured precisely, as it appears only once in the sample. It is clearly seen that the relationship d_{32} versus d_{max} is not linear. This agrees with the experiments of Zhou and Kresta [2] conducted at very low hold-up fraction ($\phi = 0.0003$) showing that the relationship d_{32} versus d_{max} was not quite linear, even though the slope did not change significantly (0.42–0.69). Pacek et al. [15] studied extensively the relationship between d_{32} and d_{max}. They also found that the d_{32} was not a constant function of d_{max} and varied randomly for the 18 cases studied. Contrary to the previously, Sprow [5] and Brown and Pitt [16] found linear relationships for d_{32} versus d_{max} with slopes 0.38 and 0.70, respectively, for disk impellers. In addition, van Heuven and Hoevenaar [17] and Giles et al. [18] reported slopes 0.50 and 0.65, respectively.

4. Conclusions

The experimental results of this work show that the impeller geometry affects the drop size distribution produced in an agitated vessel. For the same impeller diameter and width and impeller rotational speed, the drops produced by the disk impeller are smaller and more uniform in size than the ones produced by the open type ones. Plots of $\ln d_{32}$ versus $\ln N$ and of $\ln d_{max}$ versus $\ln N$ for both impellers gave straight lines. Plot of d_{32} versus d_{max} for both impellers gave relationships relationships not quite linear.

References

[1] L.L. Tavlarides, M. Stamatoudis, Adv. Chem. Eng. 11 (1981) 199.
[2] G. Zhou, S.M. Kresta, Chem. Eng. Sci. 53 (1998) 2063.
[3] A.N. Kolmogoroff, Dokl. Akad. Nauk SSSR 66 (1949) 825.
[4] J.O. Hinze, AIChE J. 1 (1955) 289.
[5] F.B. Sprow, Chem. Eng. Sci. 22 (1967) 435.
[6] J.H. Rushton, E.W. Costich, H.J. Everett, Chem. Eng. Prog. 46 (1950) 467.
[7] R.L. Bates, P.L. Fondy, R.R. Corpstein, Ind. Eng. Chem. Process Des. Dev. 2 (1963) 310.
[8] G. Zhou, S.M. Kresta, AIChE J. 42 (1996) 2476.
[9] D. Daglas, M. Stamatoudis, Chem. Eng. Technol. 23 (2000) 437.
[10] J.B. Fernandes, M.M. Sharma, Chem. Eng. Sci. 22 (1967) 1267.
[11] D.E. Brown, K. Pitt, Chem. Eng. Sci. 29 (1974) 345.
[12] A.W. Pacek, S. Chamsart, A.W. Nienow, A. Bakker, Chem. Eng. Sci. 54 (1999) 4211.
[13] L.P. Bayvel, Atomiz. Spray Technol. 1 (1985) 3.
[14] R. Shinnar, J. Fluid Mech. 10 (1961) 259.
[15] A.W. Pacek, C.C. Man, A.W. Nienow, Chem. Eng. Sci. 53 (1998) 2005.
[16] D.E. Brown, K. Pitt, Chem. Eng. Sci. 27 (1972) 577.
[17] J.W. van Heuven, J.C. Hoevenaar, Proceedings of the Fourth International Symposium on Reaction Engineering, Bruxelles, September, 1969.
[18] J.P. Giles, C. Hanson, J.G. Marsland, Proc. I.S.E.C., Amsterdam, April, 1971.